PASJ: Publ. Astron. Soc. Japan **59**, S655–S662, 2007 November 30

A Tale of Two Spicules: The Impact of Spicules on the Magnetic Chromosphere*

Bart DE PONTIEU,[1] Scott MCINTOSH,[2,3] Viggo H. HANSTEEN,[4,1] Mats CARLSSON,[4] Carolus J. SCHRIJVER,[1] Theodore D. TARBELL,[1] Alan M. TITLE,[1] Richard A. SHINE,[1] Yoshinori SUEMATSU,[5] Saku TSUNETA,[5] Yukio KATSUKAWA,[5] Kiyoshi ICHIMOTO,[5] Toshifumi SHIMIZU,[6] and Shin'ichi NAGATA[7]

[1]*Lockheed Martin Solar and Astrophysics Laboratory, Palo Alto, CA 94304, USA*
bdp@lmsal.com, schryver@lmsal.com, tarbell@lmsal.com, title@lmsal.com, shine@lmsal.com
[2]*High Altitude Observatory, National Center for Atmospheric Research, P.O. Box 3000, Boulder, CO 80307, USA*
mscott@hao.ucar.edu
[3]*Department of Space Studies, Southwest Research Institute, 1050 Walnut St., Suite 400, Boulder, CO 80302, USA*
[4]*Institute of Theoretical Astrophysics, University of Oslo, PB 1029 Blindern, 0315 Oslo Norway*
Viggo.Hansteen@astro.uio.no, Mats.Carlsson@astro.uio.no
[5]*National Astronomical Observatory of Japan, 2-21-1 Osawa, Mitaka, Tokyo 181-8588*
yoshinori.suematsu@nao.ac.jp,saku.tsuneta@nao.ac.jp, yukio.katsukawa@nao.ac.jp, kiyoshi.ichimoto@nao.ac.jp
[6]*Institute of Space and Astronautical Science, Japan Aerospace Exploration Agency, 3-1-1 Yoshinodai, Sagamihara, Kanagawa 229-8510*
shimizu.toshifumi@isas.jaxa.jp
[7]*Hida Observatory, Graduate School of Science, Kyoto University, Kurabashira, Kamitakara-cho, Takayama, Gifu, 506-1314*
nagata@kwasan.kyoto-u.ac.jp

(Received 2007 June 12; accepted 2007 August 29)

Abstract

We use high-resolution observations of the Sun in Ca II H (3968 Å) from the Solar Optical Telescope on Hinode to show that there are at least two types of spicules that dominate the structure of the magnetic solar chromosphere. Both types are tied to the relentless magnetoconvective driving in the photosphere, but have very different dynamic properties. "Type-I" spicules are driven by shock waves that form when global oscillations and convective flows leak into the upper atmosphere along magnetic field lines on 3–7 minute timescales. "Type-II" spicules are much more dynamic: they form rapidly (in ~ 10 s), are very thin (≤ 200 km wide), have lifetimes of 10–150 s (at any one height), and seem to be rapidly heated to (at least) transition region temperatures, sending material through the chromosphere at speeds of order 50–150 km s^{-1}. The properties of Type II spicules suggest a formation process that is a consequence of magnetic reconnection, typically in the vicinity of magnetic flux concentrations in plage and network. Both types of spicules are observed to carry Alfvén waves with significant amplitudes of order 20 km s^{-1}.

Key words: Sun: chromosphere — Sun: transition region

1. Introduction

The dynamics of the magnetized chromosphere are dominated by spicules (at the limb, e.g., Beckers 1968) and related flows such as mottles and fibrils (on the disk, see e.g., Hansteen et al. 2006; De Pontieu et al. 2007a, 2007b). Spicular features are also visible at the limb in many spectral lines formed at transition region (TR) temperatures (Mariska 1992; Wilhelm 2000), and recent observations suggest that much of the TR and perhaps coronal dynamics and energetics are intimately linked to spicule-like jets (McIntosh et al. 2007).

Spicules have been studied for many decades, but until recently they have remained difficult to understand because their structure and dynamics were too close to observational resolution limits (Sterling 2000). Recently, high spatial and temporal resolution observations from the ground (Swedish 1 m Solar Telescope — SST: Scharmer et al. 2003) and advanced radiative MHD simulations (e.g., Hansteen & Gudiksen 2005; Hansteen et al. 2006, 2007) have allowed us to make significant progress in our understanding of mottles and fibrils (Hansteen et al. 2006; De Pontieu et al. 2007a; Rouppe van der Voort et al. 2007; Heggland et al. 2007). Comparisons between the observations and simulations showed that active region dynamic fibrils and a subset of quiet Sun mottles are formed when photospheric oscillations and convective flows leak into the chromosphere along magnetic field lines, where they form shocks to drive jets of chromospheric plasma, as suggested by De Pontieu et al. (2004).

While our understanding of fibrils and mottles (both observed on the disk) has improved considerably, it remains unclear how or whether these features are related to spicules at the limb (e.g., Tsiropoula et al. 1994; Suematsu et al. 1995). Here we use high-resolution magnetograms, and optical and EUV images and spectra from Hinode (Ichimoto et al. 2005;

* Movies 1 and 2 are available at ⟨http://pasj.asj.or.jp/v59/sp3/59s314/⟩.

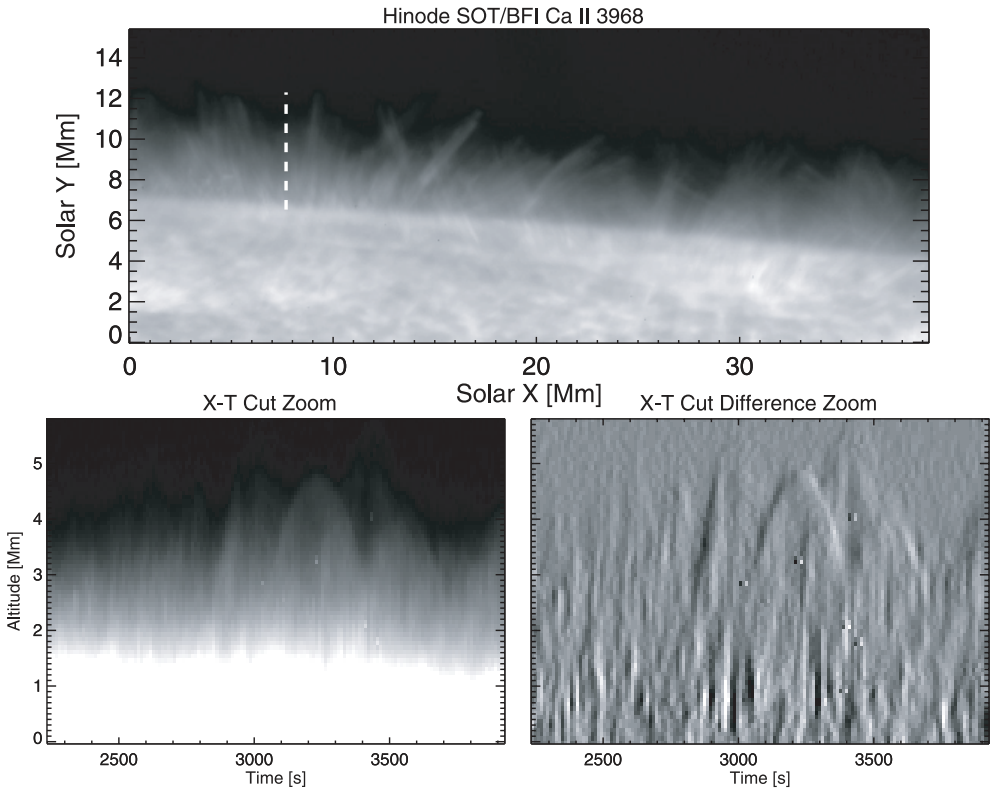

Fig. 1. The top panel shows spicules at the quiet Sun limb on 2006 November 22, in SOT/BFI Ca II H 3968 Å data. The bottom panels show space–time ("xt") plots along the location indicated by a dashed line in the top panels, for both the original data and time differenced data. The space–time plot is dominated by short-lived vertical stripes (type II spicules) and longer-lived parabolic paths (type I spicules).

Ichimoto & Solar-B Team 2005) as well as 1600 Å passband imaging from the Transition Region and Coronal Explorer (TRACE; Handy et al. 1999), to demonstrate that there are (at least) two types of chromospheric spicules. Both types are intrinsically tied to magneto–convective field evolution but are readily distinguished by their very different dynamic behavior.

Section 2 will detail the observations and analysis techniques used in this study. Section 3 discusses the results of the analysis and the potential impact of our results on our understanding of the transition region (and corona). We also pose several unresolved issues and questions in this section.

2. Observations and Data Analysis

We use a series of image sequences obtained since 2006 November with the SOT Broadband Filter Imager (BFI: Tarbell et al. 2007) in the Ca II H 3968 Å wavelength range. The Ca II H filter is fairly broad with a FWHM of 2.2 Å so that both photospheric and chromospheric emissions contribute. Carlsson et al. (2007) show that the contribution function on the disk is typically dominated by strong photospheric components, with the middle to upper chromosphere contributing only a small fraction of the emission. Off the limb, much of the emission comes from middle to upper chromospheric plasma. The time series we study have been obtained for a variety of locations: quiet Sun (QS), active region (AR), and coronal hole (CH). They have a fixed cadence between 4 and 11.2 s (with an exposure time of 0.5 s) and a spatial resolution determined by the diffraction limit of the SOT, of order 0.″16 for the Ca II H images. The pixel size is 0.″054, with a field of view varying between 1024×2048 and 2048×1024 pixels. To correct the images for dark current and miscellaneous camera artefacts (e.g., the two columns in the center which are missing in the original data), we apply the IDL routine `fg_prep.pro`, which is part of the Hinode tree of solarsoft (Tarbell et al. 2007). While the SOT correlation tracker removes most of the jitter introduced by the spacecraft, we remove the remaining slow drift of the time series by performing a rigid co-alignment of the time series. To this end we use cross-correlation techniques (from image to image) and apply the cumulative offsets to the whole time series (usually about 1 hour long). Using this technique we achieve datasets that are co-aligned to much better than one pixel from image to image.

Movies of the limb in Ca II H reveal a wealth of information on the dynamic solar chromosphere: surges, prominences, macrospicules, and spicules (see figure 1). We focus here on the spicules. Our time series show that the limb is dominated by these thin, long, and highly dynamic features. They have diameters from about 700 km (1″) down to the resolution limit of the telescope (120 km). Their maximum lengths vary from a few hundred kilometers to 10000 km with most below 5000 km. Many are seen to go up and down, whereas others show only upward motion, followed by a rapid fading from the Ca II H passband. In addition, the majority of spicules seen in our time series undergo significant

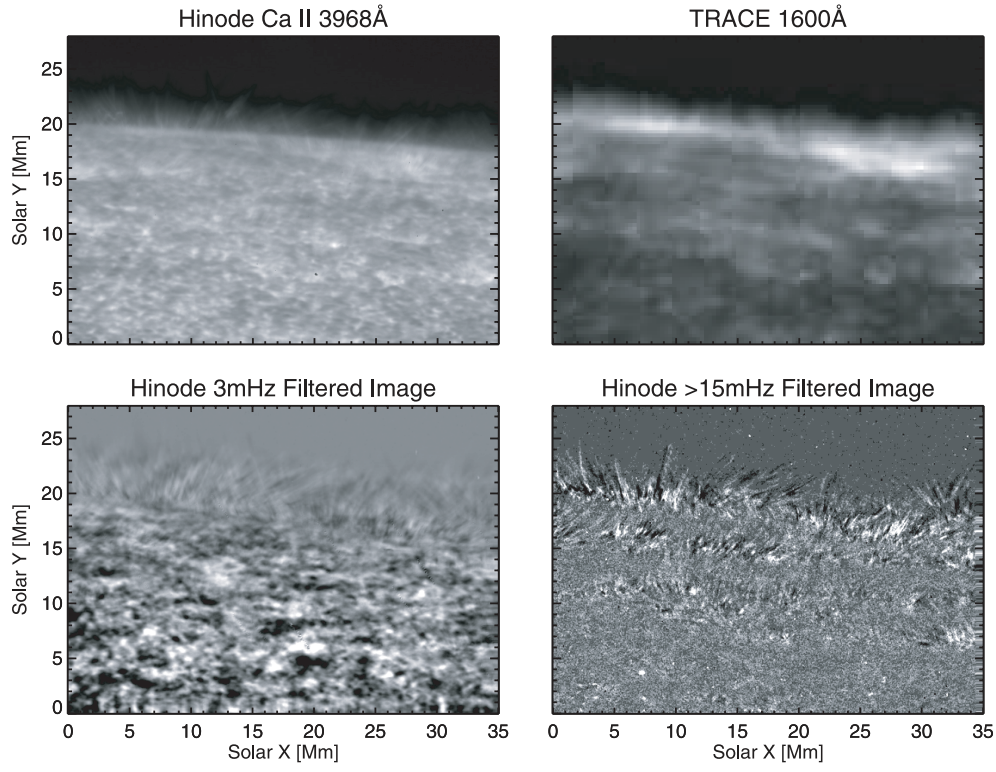

Fig. 2. Sample images from the Fourier filtered time series of SOT-BFI Ca II H 3968 Å images (top left) in the 3 mHz (bottom left) and ≥15 mHz (bottom right) passbands. These passbands isolate the two spicular species (see text). A comparison of the high frequency filtered Hinode images with those from the TRACE 1600 Å passband suggests that type II spicules and "straws" (on the disk) are associated with bright C IV transition region emission (top right).

lateral motion, i.e., motion that appears to be transverse to the long axis of the spicules. These lateral motions have been interpreted as Alfvénic motions (for more details, see De Pontieu et al. 2007c).

A visual study of the dynamic behavior of the spicules reveals that there are *at least* two different populations governed by very different time scales. To study these populations in detail, we create a Fourier filtered time series for each individual spatial pixel. The Fourier filtering is done only in time, and we apply two different filters. The first, low-frequency, filter is a Gaussian centered on 3 mHz with a width of 0.5 mHz. This filter is designed to isolate significant propagating 5 minute power off the limb. These low frequency filtered movies show the "type I" spicules: relatively slowly evolving features that typically move up and down during their lifetimes of order 3–7 minutes. A second, much more dynamic specular component is invisible in these movies because these "type II" spicules often appear or disappear within 4.8 s (which is the highest cadence we have obtained). The second filter is designed to bring out these short-lived features. It is a combination of a high-pass filter ($\geq$ 15 mHz) with a low-pass filter placed at a frequency which is 2 mHz lower than the Nyquist frequency of the time series studied. The low-pass filter is designed to remove any effects on the filtered time series from any residual jitter not removed by our co-alignment procedure.

Movies of high frequency filtered data isolate the "type II" spicules very well, both at the limb and on the disk, where they occur as "straws" predominantly in and around the chromospheric network and plage. We refer to them as "straws" on the disk since we believe the disk features have a close resemblance to the straws described by Rutten (2006, 2007).

Figure 2 shows the comparison of a Ca II H 3968 Å image (top left) with the corresponding frame from the low (bottom left) and high frequency (bottom right) filtered time series. For later reference we compare these images with a simultaneous image from the 1600 Å passband of TRACE.

The following subsections discuss the appearance of each spicule type and provide some of their basic properties.

2.1. *Type-I Spicules*

Type I spicules are dominated by dynamics on time scales of 3–7 min. They show a succession of upward and downward motion. While many undergo transverse motions during their lifetime, xt-cuts with x roughly perpendicular to the limb show that type I spicules that do not move transversely often undergo parabolic paths (bottom left panel of figure 1 and top panel of figure 3), most often with a deceleration that is not equal to solar gravity (i.e., their paths are non-ballistic, with decelerations between 50 and 400 m s^{-2}). This behavior is identical to that of AR dynamic fibrils and some QS mottles (Suematsu et al. 1995) as observed in Hα with the Swedish 1m Solar Telescope (Hansteen et al. 2006; De Pontieu et al. 2007a; Rouppe van der Voort et al. 2007). These authors measured the parabolic parameters of these fibrils/mottles and found a linear correlation between the deceleration and maximum

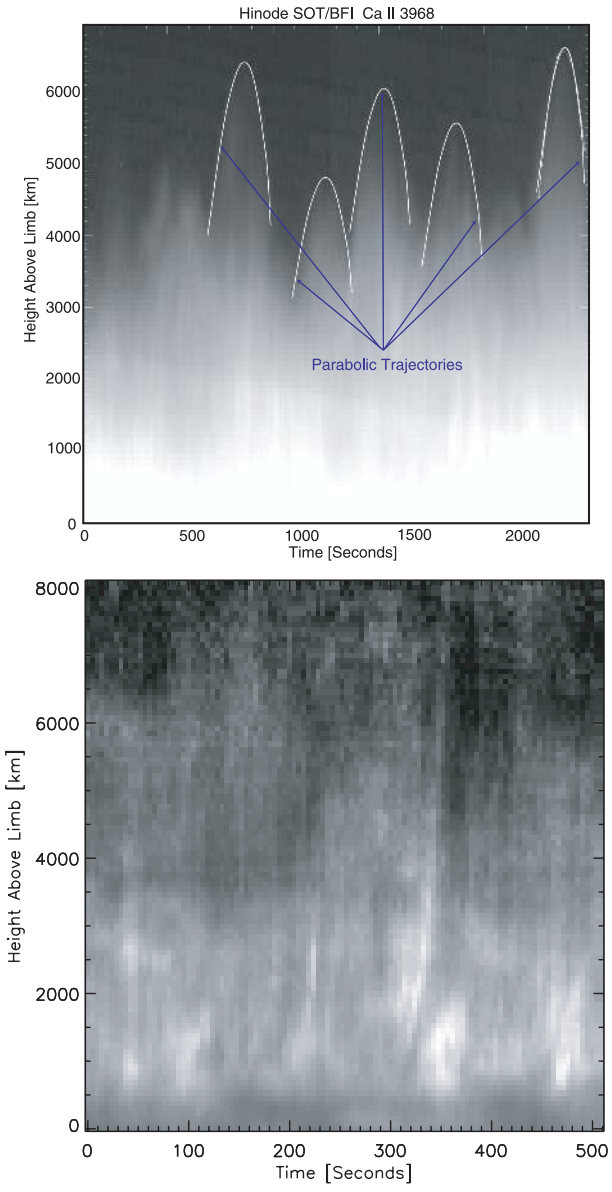

Fig. 3. The top panel shows a succession of parabolic paths taken by type I spicules in a space–time plot of Hinode/SOT Ca II H 3968 Å data with the spatial direction perpendicular to the quiet Sun limb. The bottom panel shows a space–time plot of short-lived and fast type II spicules at the coronal hole limb. At each height, the data in the bottom panel has been divided by the average brightness for that height to bring out more details at the top of the spicules. Typical for type II spicules are short-lived vertical tracks, some of which show signs of acceleration (e.g., $t = 320$ s). This figure is accompanied by two movies that illustrate the different dynamics of both spicule types. Movie 1* shows the temporal evolution of Ca II H 3968 Å images of the limb dominated by quiet Sun and weak active region with a cadence of 8 s, as taken with Hinode/SOT-BFI on 2006 November 22. Many of the spicules shown in movie 1 are type I spicules, with up- and down-motion along parabolic paths. Movie 2* shows Ca II H 3968 Å images of a coronal hole on 2007 March 19. Most spicules seen here are type II.

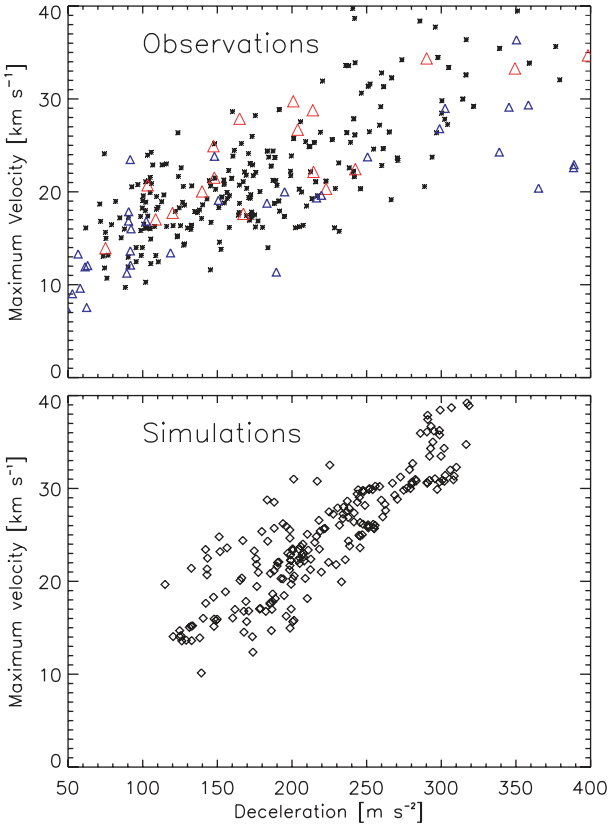

Fig. 4. Scatter plot of maximum velocity vs. deceleration for the parabolic paths of type I spicules (from Hinode/SOT Ca II H data, red triangles), quiet Sun mottles (from SST data, blue triangles), and active region fibrils (small black asterisks). The fibril data were corrected for line-of-sight projection by taking into account the viewing angle based from a magnetic field extrapolation (for details, see De Pontieu et al. 2007a). Type I spicules shows the same linear correlation as fibrils and quiet Sun mottles (the latter data is taken from, Rouppe van der Voort et al. 2007). The bottom panel shows a similar correlation for parabolic parameters of jets from numerical simulations (Hansteen et al. 2006). These jets are caused by shock waves that form when oscillations and convective motions leak into the chromosphere. The scatter in the observational data is caused by the uncertainty in line-of-sight projection which is unknown for the mottles and type I spicules, and only roughly known for the fibrils.

velocity of the paths taken by the fibrils and mottles. This linear correlation can be readily understood in terms of shock wave physics (De Pontieu et al. 2007b; Heggland et al. 2007).

Using the same technique as described in detail in De Pontieu et al. (2007a), we measured the (constant) deceleration and maximum velocity of 20 spicules that followed a parabolic path, as observed at the limb in SOT/BFI Ca II H time series. We find that the observed decelerations and maximum velocities of the type I spicules (red triangles in figure 4) cover a similar range as for the fibrils (small black asterisks), quiet Sun mottles (blue diamonds), and jets in the numerical simulations (bottom panel figure 4). In addition, they show an identical linear correlation between deceleration and maximum velocity, as illustrated in figure 4. Given these similarities and the linear correlation, it thus seems highly likely that the shockwave-driven mechanism also powers this subset (type I) of spicules observed in Ca II H at the limb. In other words, type I spicules seem to be the limb equivalents of dynamic fibrils in active regions, and of a subset of quiet Sun mottles.

In fact, on the disk these type I spicules are sometimes visible in absorption in Hinode/SOT Ca II H data as well,

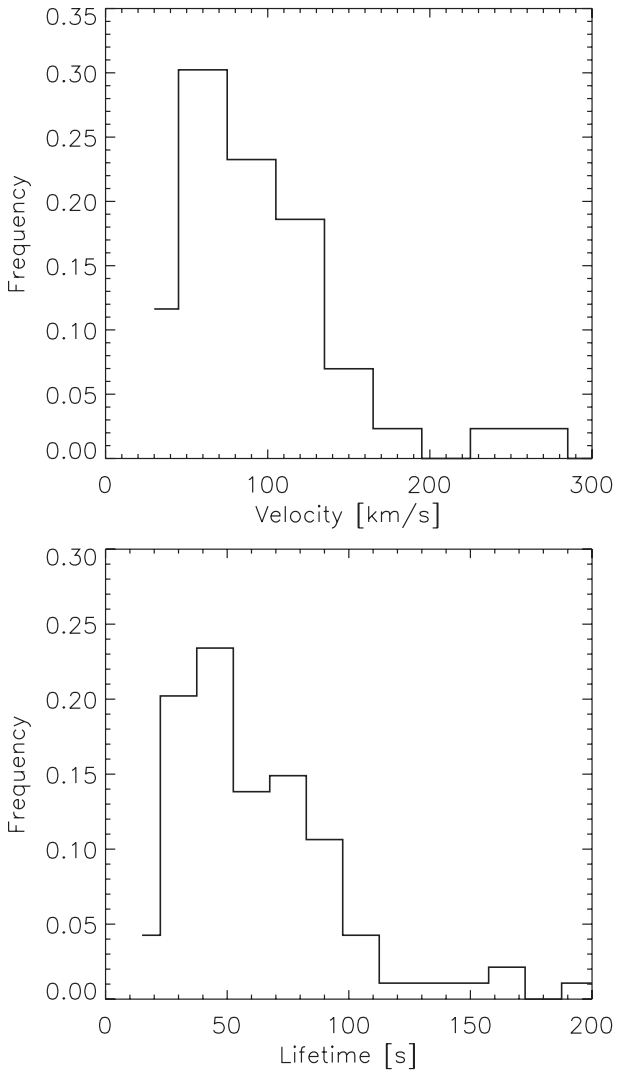

Fig. 5. Histogram of upward velocities and lifetimes of type II spicules in a coronal hole, from Ca II H 3968 Å data taken with SOT/BFI on 2007 March 19. The average lifetime is of order 45 s, with upward velocities along the type II spicules ranging between 40 and 200 km s^{-1}.

but only if the background is bright enough (plage or bright network, especially towards the limb). The broad SOT Ca II H filter with its large photospheric contributions decreases the visibility on the disk of these dark, absorbing features sometimes, but similar behavior has been seen more clearly in narrow-band Ca II H core images taken with the SST.

Type I spicules seem to be quite dominant at the active region limb, but their visibility in quiet Sun and coronal holes varies. Especially in coronal holes they are more difficult to detect in SOT/BFI Ca II H, although sometimes they seem to appear there as short and dark ($\sim$2 Mm) absorbing features against a background of bright (and longer) type II spicules.

2.2. *Type-II Spicules*

Space–time plots ("xt-cuts") of Hinode/SOT Ca II H time series at the limb (bottom panel of figure 3) and close to the network or plage reveal a second type of spicules. These type II spicules are highly dynamic, develop apparent speeds between 50–150 km s^{-1}, reach lengths between 1000 and 7000 km, and often disappear over their whole length within one or a few timesteps (5–20 s). Their lifetimes at any one height are usually between 10 and 60 s as illustrated in the bottom panel of figure 5. Their duration at any one height shows a Gaussian distribution centered at 45 s with a width of 20 s in coronal holes. In quiet Sun they are somewhat shorter-lived, with an average around 35 s at any one height. The apparent upward speeds of type II spicules range between 40 km s^{-1} and 300 km s^{-1}, with the bulk between 50–150 km s^{-1} (top panel of figure 5). This is significantly higher than type I spicules, which typically do not reach maximum velocities higher than 40 km s^{-1}. Space–time plots of type II spicules reveal that a significant number appear to be slower in during very short initial phase (see bottom panel of figure 3) and seem to accelerate as they reach greater heights towards the end of their short life.

Individual type II spicules are often weak and show up as brightness enhancements (of order 5–10% compared to the background) above a background intensity that typically shows an exponential drop-off with height with scale heights between 2 Mm (AR and QS) and 3 Mm (coronal hole). Type II spicules appear to travel upwards because of their rapid disappearance or fading at the end of their lifetime. This is clearly visible in Fourier filtered movies using the high frequency filter described before. Given the rapid appearance and disappearance, these type II spicules also dominate difference movies made by subtracting neighboring images from time series with the highest possible cadence.

Unsharp masking of SOT/BFI Ca II H images at scales of 150–200 km reveals that most type II spicules are very thin: the line-of-sight is dominated by a myriad of these features. It may well be that observed background intensity is a superposition of many type II spicules. Like type I spicules, most type II spicules undergo significant transverse motions (De Pontieu et al. 2007c).

Type II spicules are typically shorter in ARs, especially when seen on the disk as straws: they often do not become longer than 1–2 Mm. In QS they routinely reach lengths of order several megameters, and they are tallest in coronal holes. Type II spicules dominate coronal holes: many reach heights of 5000 km or more. As mentioned before, type I spicules seem to be minimally present in CHs.

What is the ultimate fate of these type II spicules and/or straws? Their extremely rapid disappearance from the Hinode/SOT Ca II H passband suggests that ionization of Ca^+ ions caused by strong heating could be occurring. This is tentatively illustrated by a preliminary comparison between the location of type II spicules and straws in Hinode/SOT Ca II H (using the high frequency filtered data) with C IV emission (formed at 100000 K) in TRACE 1600 Å. Figure 2 shows that the highest density of straws and type II spicules (bottom right panel) occurs where TRACE 1600 Å shows the largest excess brightness compared to the unfiltered SOT/BFI Ca II H image (upper right panel). Since both the TRACE 1600 Å passband and the SOT Ca II H passband are mostly dominated by photospheric or low chromospheric contributions, the excess brightness of TRACE 1600 Å points towards a significant contribution of C IV emission at the location where

the straws are the strongest and most dense. This suggests that straws and type II spicules may be heated to TR temperatures of at least 100000 K. Comparisons between Hinode/SOT Ca II H images and TRACE or Hinode/EIS-XRT spectra and images will be necessary to shed further light on the ultimate fate of type II spicules.

3. Discussion

The presence of at least two different spicule types indicates that there are several different mechanisms working on the Sun to produce spicules. This complicated picture has contributed significantly to the multitude of theoretical models and general confusion in the past regarding the cause of spicules (see, e.g., Sterling 2000). For example, there have been many conflicting reports in the literature on whether spicules fade from view or not (Beckers 1968). This discussion becomes much clearer when taking into account the different properties of both spicule types: type I's move up and down, whereas type II's fade.

The first spicule driving mechanism is now fairly well understood. Photospheric oscillations and convective motions can leak into the chromosphere along magnetic flux concentrations (i.e., low plasma β environment), where they form shock waves that drive jets of plasma upwards (De Pontieu et al. 2004). These jets fall back down after a few minutes, so that the top of the jet tracks a parabolic path. The constant deceleration and maximum velocity of the parabolic motion are linearly correlated because of shockwave physics (Heggland et al. 2007). This mechanism seems to drive the type I spicules we see here and also causes much of the dynamics seen in Hα on the disk around and above plage regions (Hansteen et al. 2006; De Pontieu et al. 2007a). It has also been associated with a subset of quiet Sun mottles seen in Hα on the disk (Rouppe van der Voort et al. 2007).

Advanced radiative MHD simulations in two and three dimensions reproduce the observed parabolic tracks, decelerations, and maximum velocities very well (Hansteen et al. 2006; De Pontieu et al. 2007a). They show that velocities of order 10–40 km s^{-1} can be expected, and that these jets do not get heated out of the Ca II H passband (Langangen et al. 2007). The lifetime of these jets is set by the inclination of the magnetic field in the photosphere and low chromosphere: significantly inclined field lowers the acoustic cutoff frequency and allows leakage of the underlying wave spectrum of the photosphere [the dominant $\sim$5 min of the p-modes, see also Jefferies et al. (2006); McIntosh & Jefferies (2006)]. Regions where the field is more vertical will be dominated by the chromospheric acoustic cutoff frequency (3 min): the energetic p-modes cannot leak upward, with shorter and shorter-lived type I spicules as a result. The effect of the inclination of the magnetic field on the wave leakage may help explain why type I spicules are difficult to observe in coronal holes. The magnetic field in coronal holes is more unipolar so that the overall direction of the field is more vertical (since it lacks much of the opposite polarity in close proximity that both QS and AR have). This could lead to less leakage of p-modes, and shorter, less energetic type I spicules as a result. It is also possible that type I spicules are harder to observe because of radiative transfer effects, caused by the different thermodynamic conditions in coronal holes.

Comparisons with numerical simulations show that the mechanism that drives type I spicules does not produce jets with (real or apparent) speeds above 50 km s^{-1} or rapid fading caused by heating to TR temperatures such as we seem to observe in the type II spicules (Hansteen et al. 2006; De Pontieu et al. 2007a; Langangen et al. 2007). So what drives type II spicules and/or straws? An obvious candidate for the driver of type II spicules is reconnection, which has been invoked as a driver for spicules in the past, usually as a result of the interaction between photospheric flux concentrations of opposite polarity (e.g., Uchida 1969; Takeuchi & Shibata 2000; Moore et al. 1999; Tsiropoula & Tziotziou 2004; Tziotziou et al. 2003, 2004; Sterling 2000). Perhaps reconnection of network and/or plage fields with the turbulent magnetic field on granular scales (for which there is now significant evidence, e.g., Trujillo-Bueno et al. 2004; Lites et al. 2007) is driving much of the type II spicular activity? Some of the taller jets we see in our Ca II H data seem to be associated with twisting motions, which may be indicative of this type of reconnection. However, it is not clear at this stage how dominant these kinds of events are at the limb. In addition, it is not (yet?) clear whether such a scenario could explain the presence of straws in the center of strong plage regions, which are observed to be mostly unipolar with Hinode/SOT-NFI magnetograms. Perhaps these straws (and some type II spicules) are caused by the dissipation of currents (and subsequent heating of plasma) caused by the continual braiding of the field? It is interesting to note that our space–time plots of type II spicules (bottom panel, figure 3) show strong similarities with similar cuts along so-called penumbral micro-jets described by Katsukawa et al. (2007). The latter seem to be caused by reconnection at tangential discontinuities of the magnetic field between neighboring penumbral filaments with similar polarity, but different field orientations. Such discontinuities can also be expected above plage regions because the relentless magnetoconvective forcing of photospheric flux concentrations shuffles the magnetic field significantly, especially at greater heights (see, e.g., van Ballegooijen et al. 1998). It is not yet fully clear whether this formation mechanism is compatible with the geometry and apparent field-aligned flows of straws/type II spicules (see, e.g., Tarbell et al. 1999), especially given the apparent heating of plasma along the whole spicule. Detailed numerical studies (along the lines of, e.g., Sterling et al. 1993) with more advanced chromospheric radiative transfer calculations will be necessary to determine what kind of heat deposition (and over which height range) is necessary to produce the thermal and dynamic properties of straws and/or type II spicules. The work of Sterling et al. (1993) suggests that only a small subset of solutions in which significant energy is deposited in the middle chromosphere come close to producing features with speeds of 50–100 km s^{-1} that reach TR temperatures above 20000 K.

The presence of straws has been described before by Rutten (2007) who used observations on the disk with the Dutch Open Telescope in La Palma to describe their morphology and association with the network. How do they relate to features in other chromospheric passbands? We have also

seen straws in Hα linecenter observations made with the SST, although at significantly reduced contrast. In the SST disk data, the straws are often obscured by fibrils and mottles, which appear as dark features in Hα. Preliminary comparisons of SOT Ca II H and Hα linecenter images at the limb show that a majority of Ca II H features also show up in Hα, with the exception of some of the shorter type II spicules that appear at lower heights where Hα linecenter shows little contrast. Detailed analysis of straws in different chromospheric lines will be necessary to disentangle the complicated appearance of spicules and their disk counterparts, which has been a long-standing source of confusion (Grossmann-Doerth & Schmidt 1992). Such an analysis will also be able to pin down whether all of the observed velocities are caused by real mass motions. This is clearly the case for type I spicules and fibrils/mottles as shown by comparisons to spectra (Langangen et al. 2007). Similar work will be necessary for the extremely thin type II spicules and straws with their high apparent velocities of 50–150 km s^{-1}. Given the very small spatial diameters of type II spicules, it is quite possible that previous observations with temporal and spatial resolution of order 30 s and 0.″5–1″ have missed most of the dynamics of the type II spicules, and have instead interpreted a superposition of many type II spicules as one spicule, or perhaps even as a background chromosphere.

What is the impact of all of these spicules on the transition region and corona? How do the different types of spicules impact the TR? Do type I spicules just move the preexisting TR emission up and down (see, e.g., de Wijn & De Pontieu 2006), or are they also associated with heating to TR temperatures (perhaps less likely)? Does a significant fraction of type II spicules get heated to 100000 K as is suggested by our comparison with TRACE C IV data? Are type II spicules the dominant source of heating in the magnetized chromosphere (or even corona)? Are type II spicules signs of chromospheric evaporation? Does a small but significant fraction of the type II spicules get heated to coronal temperatures? These are some of the unresolved questions which are of great importance since they may well shed light on the dominant heating mechanisms of both the chromosphere and corona, as suggested previously by Athay and Holzer (1982), Athay (2000), Withbroe (1983), and Budnik et al. (1998). The access to extremely high resolution Hinode data has made the resolution of these issues within view, for the first time. Comparisons with high-resolution EUV and UV spectra and imaging will help reveal whether reconnection dominates the jets visible in UV/EUV (Wilhelm 2000) or whether, for example, electron beam heating or conductive heating from the corona has any role to play in the formation of type II spicules. For example, such UV data has been used recently by McIntosh et al. (2006, 2007) to suggest that reconnection-driven jets can explain the spatial distribution on supergranular scales of redshifts and blueshifts in UV spectral lines that are formed at TR temperatures.

Our observations indicate that both wave-driven jets and reconnection-driven jets are prevalent in the chromosphere. The relative importance of these mechanisms seems to vary significantly between active regions, quiet Sun, and coronal holes. Many of these jets undergo vigorous transverse motions that are caused by Alfvén waves. Preliminary estimates suggest that these Alfvén waves carry an energy flux that may be of importance for the local energy balance, and once they reach the corona, can play a significant role in the heating of the quiet Sun corona and acceleration of the solar wind (De Pontieu et al. 2007c). The role of Alfvén waves in the formation of spicules or the solar wind has been previously discussed by, e.g., Hollweg et al. (1982) and Kudoh and Shibata (1999), although such waves had not been previously observed in spicules.

We are grateful to the Hinode team for their efforts in the design, building and operation of the mission. Hinode is a Japanese mission developed and launched by ISAS/JAXA, with NAOJ as domestic partner and NASA and STFC (UK) as international partners. It is operated by these agencies in co-operation with ESA and NSC (Norway). SOT was developed jointly by NAOJ, LMSAL, ISAS/JAXA, NASA, HAO and MELCO. B.D.P. was supported by by NASA contracts NNG06GG79G, NNG04-GC08G, NAS5-38099 (TRACE) and NNM07AA01C (HINODE). SWM was supported by grants from the NSF (ATM-0541567) and NASA (NNG05GM75G, NNG06GC89G).

References

Athay, R. G. 2000, Sol. Phys., 197, 31
Athay, R. G., & Holzer, T. E. 1982, ApJ, 255, 743
Beckers, J. M. 1968, Sol. Phys., 3, 367
Budnik, F., Schröder, K.-P., Wilhelm, K., & Glassmeier, K.-H. 1998, A&A, 334, L77
Carlsson, M., et al. 2007, PASJ, 59, S663
De Pontieu, B., et al. 2007b, in ASP Conf. Ser., 368, Coimbra Solar Physics Meeting on the Physics of Chromospheric Plasmas, ed. P. Heinzel, I. Dorotovic, & R. J. Rutten (San Francisco: ASP), 65
De Pontieu, B., et al. 2007c, Science submitted
De Pontieu, B., Erdélyi, R., & James, S. P. 2004, Nature, 430, 536
De Pontieu, B., Hansteen, V. H., Rouppe van der Voort, L., van Noort, M., & Carlsson, M. 2007a, ApJ, 655, 624
de Wijn, A. G., & De Pontieu, B. 2006, A&A, 460, 309
Grossmann-Doerth, U., & Schmidt, W. 1992, A&A, 264, 236
Handy, B. N., et al. 1999, Sol. Phys., 187, 229
Hansteen, V. H., Carlsson, M., & Gudiksen, B. 2007, in ASP Conf. Ser., 368, Coimbra Solar Physics Meeting on the Physics of Chromospheric Plasmas, ed. P. Heinzel, I. Dorotovic, & R. J. Rutten (San Francisco: ASP), 107
Hansteen, V. H., De Pontieu, B., Rouppe van der Voort, L., van Noort, M., & Carlsson, M. 2006, ApJ, 647, L73
Hansteen, V. H., & Gudiksen, B. 2005, in Proc. Solar Wind 11-SOHO 16, Connecting Sun and Heliosphere, ed. B. Fleck & T. H. Zurbuchen, ESA SP-592 (Noordwijk: ESTEC), 483
Heggland, L., De Pontieu, B., & Hansteen, V. H. 2007, ApJ, 666, 1277
Hollweg, J. V., Jackson, S., & Galloway, D. 1982, Sol. Phys., 75, 35

Ichimoto, K., et al. 2005, in Proc. Chromospheric and Coronal Magnetic Fields, ESA SP-596, 81
Ichimoto, K., & Solar-B Team 2005, J. Kor. Ast. Soc., 38, 307
Jefferies, S. M., McIntosh, S. W., Armstrong, J. D., Bogdan, T. J, Cacciani, A., & Fleck, B. 2006, ApJ, 648, L151
Katsukawa, Y., et al. 2007, PASJ, 59, S577
Kudoh, T., & Shibata, K. 1999, ApJ, 514, 394
Langangen, O., Carlsson, M., Rouppe van der Voort, L., Hansteen, V., & De Pontieu, B. 2007, ApJ in press
Lites, B., et al. 2007, PASJ, 59, S571
Mariska, J. T. 1992, The Solar Transition Region (Cambridge: Cambridge University Press)
McIntosh, S. W., Davey, A. R., & Hassler, D. M. 2006, ApJ, 644, L87
McIntosh, S. W., Davey, A. R., Hassler, D. M., Armstrong, J. D., Curdt, W., Wilhelm, K., & Lin, G. 2007, ApJ, 654, 650
McIntosh, S. W., & Jefferies, S. M. 2006, ApJ, 647, L77
Moore, R. L., Falconer, D. A., Porter, J. G., & Suess, S. T. 1999, ApJ, 526, 505
Rouppe van der Voort, L. H. M., De Pontieu, B., Hansteen, V. H., Carlsson, M., & van Noort, M. 2007, ApJ, 660, L169
Rutten, R. J. 2006, in ASP Conf. Ser., 354, Solar MHD Theory and Observations: A High Spatial Resolution Perspective ed. H. Uitenbroek, J. Leibacher, & R. F. Stein (San Francisco: ASP), 276
Rutten, R. J. 2007, in ASP Conf. Ser., 368, Coimbra Solar Physics Meeting on the Physics of Chromospheric Plasmas, ed. P. Heinzel, I. Dorotovic, & R. J. Rutten (San Francisco: ASP), 21
Scharmer, G. B., et al. 2003, Proc. SPIE., 4853, 34
Sterling, A. C. 2000, Sol. Phys., 196, 79
Sterling, A. C., Shibata, K., & Mariska, J. T. 1993, ApJ, 407, 778
Suematsu, Y., Wang, H., & Zirin, H. 1995, ApJ, 450, 411
Takeuchi, A., & Shibata, K. 2000, ApJ, 546, L73
Tarbell, T., et al. 2007, Sol. Phys. submitted
Tarbell, T., Ryutova, M., Covington, J., & Fludra, A. 1999, ApJ, 514, L47
Trujillo-Bueno, J., Shchukina, N., & Asensio Ramos, A. 2004, Nature, 430, 326
Tsiropoula, G., Alissandrakis, C. E., & Schmieder, B. 1994, A&A, 290, 285
Tsiropoula, G., & Tziotziou, K. 2004, A&A, 424, 279
Tziotziou, K., Tsiropoula, G., & Mein, P. 2003, A&A, 402, 361
Tziotziou, K., Tsiropoula, G., & Mein, P. 2004, A&A, 423, 1133
Uchida, Y. 1969, Sol. Phys., 21, 128
van Ballegooijen, A. A., Nisenson, P., Noyes, R. W., Löfdahl, M. G., Stein, R. F., Nordlund, Å., & Krishnakumar, V. 1998, ApJ, 509, 435
van Noort, M., Rouppe van der Voort, L., & Löfdahl, M. G. 2005, Sol. Phys., 228, 191
Wilhelm, K. 2000, A&A, 360, 351
Withbroe, G. 1983, ApJ, 267, 825